



Published in final edited form as:

*Mol Pharm.* 2013 March 4; 10(3): 988–998. doi:10.1021/mp300436c.

## Evidence of Oral Translocation of Anionic G6.5 Dendrimers in Mice

Giridhar Thiagarajan<sup>‡,†</sup>, Shraddha Sadekar<sup>§,†</sup>, Khaled Greish<sup>§,†,1</sup>, Abhijit Ray<sup>§,†</sup>, and Hamidreza Ghandehari<sup>§,†,†,\*</sup>

<sup>‡</sup>Department of Bioengineering, Nano Institute of Utah, University of Utah, Salt Lake City, Utah 84112, United States

<sup>§</sup>Department of Pharmaceutics and Pharmaceutical Chemistry, Nano Institute of Utah, University of Utah, Salt Lake City, Utah 84112, United States

<sup>†</sup>Utah Center for Nanomedicine, Nano Institute of Utah, University of Utah, Salt Lake City, Utah 84112, United States

### Abstract

Development of carrier systems to improve oral bioavailability and target drugs to specific sites continues to be an unmet need. The goal of this study was to evaluate the potential of anionic generation (G) 6.5 poly(amido amine) (PAMAM) dendrimers in oral drug delivery by assessing their *in vivo* oral translocation. G6.5-COOH dendrimers were characterized for their physicochemical characteristics and acute oral toxicity was assessed in CD-1 mice. The dendrimers were labeled with <sup>125</sup>I and their stability evaluated. Oral bioavailability was assessed in the same mouse model. Investigation of the radioactivity profile in plasma, revealed presence of both large and small molecular weight compounds. Detailed area under the curve analysis suggests an effective 9.4% bioavailability of radiolabeled marker associated with G6.5-COOH. Results reported here suggest the potential of dendrimers in permeating gastrointestinal barriers *in vivo*.

### Keywords

Polymer therapeutics; Oral translocation; bioavailability; PAMAM dendrimers; Drug delivery

## INTRODUCTION

Delivering drugs using macromolecular carriers can overcome non-specific toxicity associated with small molecular weight compounds<sup>1</sup>. Macromolecular therapeutics such as polymer-drug conjugates are known to circulate longer in blood<sup>2, 3</sup> by virtue of their size, in turn reducing the need to administer larger than required doses. These delivery systems can also be fine-tuned to release the drug payload at specific sites<sup>4</sup>, which can further reduce

\*Corresponding author: Hamidreza Ghandehari, Utah Center for Nanomedicine, Nano Institute of Utah, University of Utah, Salt Lake City, UT 84112, USA. Tel: +(001) 801 587 1566. Fax: +(001) 801 585 0575. hamid.ghandehari@pharm.utah.edu.

<sup>1</sup>Present address: Department of Pharmacology & Toxicology, Otago School of Medical Sciences, University of Otago, Dunedin, New Zealand

**SUPPORTING INFORMATION.** Contains figures and tables representing: 1) Synthetic scheme for the radiolabeling of G6.5-COOH dendrimers, 2) Control PD-10 experiments with Bolton-Hunter (<sup>125</sup>I) reagent in plasma and urine, 3) Radioactivity profile of urine from CD-1 mice orally administered with radiolabeled G6.5-COOH over time as analyzed by size exclusion chromatography, 4) Radioactivity profile in plasma and urine from CD-1 mice *i.v.* administered with G6.5-COOH as analyzed by size exclusion chromatography, 5) Clinical parameters evaluated for signs of toxicity in CD-1 mice. This material is available free of charge via the Internet at <http://pubs.acs.org>

toxic side effects. Macromolecular drug conjugates passively accumulate into sites of inflammation and disease over time improving efficacy<sup>5, 6</sup>. From an oral drug delivery perspective, hydrophilic polymers can substantially increase the solubility of hydrophobic drugs, and if designed appropriately can enhance their trans-epithelial transport. Considering the advantages of macromolecular carriers, it would be beneficial to be able to deliver such systems orally.

Size and surface charge are two important parameters that are known to play crucial roles in oral absorption of polymeric systems *in vivo*<sup>7-9</sup>. Cationic polymers such as chitosan, for example, are known to increase paracellular transport by interaction with tight junctions and associated proteins (e.g., occludin, ZO-1 and actin cytoskeleton)<sup>10-12</sup>. Anionic systems, on the other hand, influence changes in intracellular calcium concentration thereby initiating a cascade of events ultimately leading to contraction of the acto-myosin filaments, and tight junction opening<sup>13-16</sup>. Although considerable progress has been made, the limited oral bioavailability exhibited by macromolecular systems restricts their further use.

Dendrimers are unique polymers that have a branched architecture and nanoscale dimensions<sup>17, 18</sup>. Step-wise growth of these branches confers a compact structure to the polymers. Multiple terminal ends of these branches can be suitably functionalized to carry a large drug payload<sup>19-23</sup>. An important characteristic of the dendrimers is that size and surface charge of these constructs can be tailored precisely<sup>18, 20, 24</sup>. Dendrimer-drug conjugates demonstrate distinct advantages over their free drug counterparts in terms of efficacy<sup>18, 25, 26</sup>, reduced systemic toxicity<sup>27</sup> and differential biodistribution patterns<sup>28-30</sup>. Since the first report of trans-epithelial transport of dendrimers in everted sac model systems<sup>31</sup>, much progress has been made in understanding the influence of physicochemical characteristics of these polymers on permeability, as well as potential mechanisms of action of translocation.<sup>31-39</sup> These studies were largely limited to an *in vitro* setting however, which does not capture the dynamic complexities presented *in vivo*, such as the acidic environment of the gastrointestinal (GI) tract, enzymatic activity of the small intestine, GI transit time, presence of mucus layer coating the intestinal epithelium, dilution of compounds in the lumen, rapid clearance and presence of immune factors such as M-cells, etc. We present here, to the best of our knowledge for the first time, results from the *in vivo* evaluation of oral translocation of radiolabeled PAMAM dendrimers across the epithelial barrier of the gut. The ultimate goal is to design an oral drug carrier that would deliver macromolecular chemotherapeutics to the systemic circulation. In order to do so it was first necessary to identify a dendrimer that was non-toxic and showed appreciable oral absorption. Earlier studies revealed serious hematological complications associated with amine-terminated PAMAM dendrimers<sup>40</sup> and hence their use in this study was not pursued. Among the anionic dendrimers, G6.5-COOH was chosen based on its *in vivo* safety profile<sup>40</sup> and favorable size characteristics as a multifunctional platform. Initially, G6.5-COOH dendrimer was evaluated for acute toxicity after oral administration in an immune competent mouse model. Once safety was determined, oral bioavailability of the carrier was assessed in the same animal model.

## EXPERIMENTAL SECTION

### Preparation and characterization of PAMAM dendrimers

Generation (G) 6.5 PAMAM dendrimers were fractionated and characterized as previously described<sup>40</sup>. Briefly, G6.5 PAMAM dendrimers with ethylene diamine core were purchased from Sigma (St. Louis, MO). Dendrimer samples were further fractionated by a preparative Sephadex Hiload 75 size exclusion column (GE Healthcare Biosciences, Piscataway, NJ) as necessary to remove small molecular weight impurities. All dendrimers were characterized at physiologically relevant pH by dynamic light scattering (DLS) on a DAWN HELEOS II

(Wyatt Technologies, Santa Barbara, CA), at a concentration of 5 mg/ml and their zeta potential recorded on a Malvern Zetasizer (Malvern Instruments Inc., Westborough, MA) at a concentration of 10 mg/ml in triplicates. Zeta potential was measured at pH 7.4 (not buffered). In addition PAMAM dendrimers were characterized by high performance liquid chromatography (HPLC) (Agilent Technologies, Santa Clara, CA) on a C18 (4.6 × 250 mm, 5 µm) column (Waters, Milford, MA) in an acetonitrile: water buffer (27:73) with 0.14% trifluoro acetic acid, and size exclusion chromatography (SEC) on an analytical Superose 6 10/300 GL column (GE Healthcare Biosciences, Piscataway, NJ). Elution buffer was PBS: Acetonitrile (80:20) with 0.1% sodium azide.

## Animals

All oral acute toxicity studies were carried out in 4–6 weeks old female CD-1 mice weighing about 25 g. Oral bioavailability studies were performed in the same CD-1 mouse model. *In-situ* stability studies were carried out in female Sprague Dawley (SD) rats weighing about 150–200 g. Both strains were purchased from Charles River Laboratories (Boston, MA) and used strictly according to the rules and guidelines of the University of Utah Institutional Animal Care and Use Committee. Animals were fed their usual diet during the course of all studies.

## Oral acute toxicity

In order to exclude local toxicity of dendrimers as the cause of increased permeation resulting in enhanced oral bioavailability, an acute toxicity study after oral administration of G6.5 PAMAM dendrimer was conducted using CD-1 mice (n=5). 1 mg/kg dose of dendrimer was prepared in a total volume of 0.2 ml/mice with physiological saline. Samples were filtered through 0.2 µm filters and administered by oral gavage using appropriately sized curved feeding needles. To exclude the presence of endotoxin in nanoparticle samples, an endpoint LAL assay (Lonza, Basel, Switzerland) was performed according to the manufacturer's instructions. Immediately after administration, animals were observed for 30 min for post injection reaction. Animal weight was recorded and systemic clinical observations for signs of toxicity such as unusual locomotion, bleeding in any orifice, ruffling of fur/skin, lacrimation/ redness of the eye, vasodilation, vasoconstriction, coldness of body, etc. <sup>40</sup> were carried out twice daily for a period of 10 days. Unless animals showed signs of toxicity (greater than 10% animal weight loss consistently for more than 2 days or other clinical signs of toxicity (Supplementary Table 1)) the acute toxicity study progressed to completion (10 day period). Ten days after injection, mice were individually euthanized using 70% CO<sub>2</sub> in oxygen, with euthanasia confirmed by lack of breathing for 30s. Blood was taken via inferior vena cava (IVC) stick, and drawn into a heparinized syringe through a 23G needle and deposited into a blood tube. Blood samples were examined for clotting and/or hemolysis upon collection. Organs (heart, lungs, liver, spleen, kidney, and GI) were removed, weighed and % weight of organ to total body weight calculated to determine organ atrophy/hypertrophy in response to dendrimer injection. Complete blood counts (CBC) were performed within two hours of blood collection using a CBC-DIFF (Heska, Loveland, CO) blood count analyzer. Following CBC, samples were centrifuged at 10,000 rpm for 2.5 minutes. The collected serum samples were used to measure blood urea nitrogen (BUN), creatinine, aspartate aminotransferase (AST), alanine aminotransferase (ALT), total bilirubin, total protein and albumin using a DRI-CHEM (Heska, Loveland, CO) veterinary blood chemistry analyzer to examine kidney and liver toxicity.

## Radiolabeling and characterization of dendrimers

G6.5-COOH PAMAM dendrimers were radiolabeled as previously reported<sup>41</sup>. Briefly, Carboxyl terminal groups were initially modified with ethylene diamine (1:2) using N-Hydroxysuccinimide/ ethyl (dimethylaminopropyl) carbodiimide reagents to facilitate

further attachment to  $^{125}\text{I}$  radiolabeled Bolton-Hunter reagent (American Radiolabeled Chemicals, Inc., St. Louis, MO). About 10mg of dendrimers were mixed separately (1:1) with  $^{125}\text{I}$  labeled Bolton-Hunter reagent (~0.5 mCi) under ice. Radiolabeling reaction (Supplementary Figure 1) was performed in borate buffer (pH 8.5) over 4h. The progression of the radiolabeling was monitored by thin layer chromatography (Solvent system: 10% methanol in chloroform). The reaction was then dialyzed in a 1000 MW cutoff dialysis membrane (Spectrum Laboratories, Inc., Rancho Dominguez, CA) against a 0.9% saline solution for 48h. All samples were fractionated on a size exclusion PD-10 column (GE Healthcare, Piscataway, NJ) before use. Radiolabeled dendrimers were characterized on a size exclusion PD-10 column. Columns were initially washed with 10 ml of saline, then 2  $\mu\text{l}$  of the sample was loaded onto the column and the initial 2 ml of saline was discarded as void volume. Subsequently 0.5 ml fractions were collected up to a volume of 10 ml and radioactivity in each fraction was read on the  $\gamma$ -counter (Canberra, Meriden, CT). A line graph was plotted between % of radioactivity recovered and volume (in ml) using Microsoft's Excel (Redmond, WA).

### Stability of radiolabeled dendrimers in simulated gastric and intestinal conditions

10ml of simulated gastric fluid (Ricca Chemical Company, Arlington, TX) containing 32 mg of porcine pepsin enzymes (Sigma, St. Louis, MO) and 10 ml of simulated intestinal fluid (Ricca Chemical Company, Arlington, TX) with 100 mg of porcine pancreatin enzymes (Sigma, St. Louis, MO) were prepared freshly according to US pharmacopeia<sup>42</sup>. Radiolabeled G6.5 dendrimers were incubated in the prepared solutions at 37° C with constant stirring. About 30,000–40,000 CPM of radioactive dendrimer was added into the test solution. It was ascertained that the sample volume constituted less than 10% of the total test solution. 200  $\mu\text{l}$  samples were collected at each time point (1h, 4h, 12h and 24h) and loaded on a PD-10 column. Size exclusion samples were processed as mentioned in the previous section. Control experiment included radiolabeled dendrimers and  $^{125}\text{I}$  mixed in test solution and immediately run on PD-10 as an equivalent of 0 min.

### *In-situ* stability

In order to evaluate the stability of radiolabeled dendrimers, intestinal secretions was collected from sacrificed CD-1 mice by flushing 2ml of saline slowly through an incision in the duodenal region and the secretions were collected from an outlet created right before the cecum. Collected solution was immediately used for evaluating the stability of radiolabeled G6.5-COOH. Procedures similar to the one described in the earlier stability section were employed. Radiolabeled G6.5 dendrimers with radioactivity of about 50,000 CPM was incubated in the solution. Results were plotted as % of radioactivity recovered vs. Volume.

*In-situ* loop perfusion experiments were performed in SD rats (n=3). Anesthesia was induced with 4%, and maintained throughout the procedure with 2% isoflurane. Once anesthetized a minimal cut was made in the abdominal region. A catheter was introduced into the duodenum by a small incision and the catheter was secured with surgical sutures. Similarly an outlet was created in the jejunum using plastic tubing to ensure free flow. Then the system was flushed with 20ml of saline. After flushing the outlet was closed using sutures. Radiolabeled G6.5-COOH sample (~150,000 CPM/mice) was introduced into the loop by injection using a syringe in 2ml volume. Animals were closely monitored throughout the procedure. At the end of 2h animals were sacrificed and sample retrieved from the loop. Size exclusion columns were run on the sample as described before. Results were plotted as % of radioactivity recovered vs. Volume.

CD-1 mice serum purchased from Charles River Laboratories (Wilmington, MA) was used to study the stability of radiolabeled dendrimers. Mouse serum was mixed with saline (1:1)

and approximately 40,000 CPM of radiolabeled G6.5-COOH was incubated in the solution. The samples were kept at 37° C under constant stirring. At the end of 24h sample was spun down at 3500 rpm for 10 min. Plasma was loaded on a size exclusion column as described earlier. <sup>125</sup>I was used as a control sample. Results were plotted as % of total CPM vs. Volume.

### ***In vivo* oral bioavailability**

CD-1 mice (n=5) were used for the oral bioavailability studies. Dendrimer samples were prepared in physiological saline (0.2 ml/mouse). A dose of 1 mg/kg of non-labeled mixed with the radiolabeled G6.5 dendrimers (~100,000 CPM/mice) was administered by oral gavage. Each mouse was housed in a separate metabolic cage that facilitated collection of separate stool and urine samples. After 4h, mice were euthanized using CO<sub>2</sub> gas. Blood was taken via inferior vena cava (IVC) stick, and drawn into a heparinized syringe through a 23G needle. All major organs were collected separately. The carcass was also collected to boost recovery of entire administered dose. Radioactivity in each organ was read on a  $\gamma$ -counter. Bioavailability was calculated as a percentage of injected doses based on the dendrimer's accumulation in blood, liver, heart, lungs, spleen, kidneys, thyroid, urine and brain. Radioactivity in the gastrointestinal tract and stool was not considered as orally bioavailable but still measured for complete recovery of administered dose.

To analyze radioactivity profile in plasma, 3 mice per group were used, a higher radioactive dose of ~500,000 CPM/mouse was administered orally and mice were sacrificed at 1h and 4h. At these time points the blood was collected in mini centrifuge tube and spun down at 3500 rpm for 10min. The plasma was then loaded on a size exclusion PD-10 column (procedure as mentioned in earlier section). Similarly, urine sample from each animal was also loaded on a size exclusion PD-10 column. Results were plotted as % radioactivity recovered vs. Volume. Control experiments included externally mixing G6.5COOH-<sup>125</sup>I and Na<sup>125</sup>I with urine and serum from mice to validate the size exclusion methods.

Radiolabeled G6.5-COOH (~1 million CPM/mice) was injected intravenously to CD-1 mice (n=1) by tail vein injection. Mouse was housed in a metabolic cage and after 4h sacrificed. Plasma and urine collected from animals were run on a PD-10 column. Results of the urine and plasma profiles were plotted as % of radioactivity recovered vs. Volume.

### **Area under the curve (AUC) analysis**

GraphPad Prism 5.01 software (GraphPad Software, Inc., La Jolla, CA) was used to calculate the area under the curve (AUC) for all the size exclusion radioactivity profiles generated. The software generated a % of area under the two major peaks that were detected corresponding to small and large molecular weight fractions. The percentages of area under the curve were represented for all size exclusion profiles along with the volume range (ml) for each peak to give a sense of the distribution of each species in the sample.

### **Statistical analysis**

Statistical differences were analyzed by a one-way ANOVAs test with Bonferroni's correction using GraphPad Prism 5.01 software (GraphPad Software, Inc., La Jolla, CA). Significant difference was defined as \* P < 0.05, \*\* P < 0.01 and \*\*\* P < 0.0001.

## **RESULTS**

### **Physiochemical characterization of G6.5-COOH dendrimers**

G6.5-COOH dendrimers were fractionated as necessary to remove small molecular weight impurities and characterized for size and charge by dynamic light scattering and zeta



potential respectively (Table 1). The size distribution of G6.5-COOH was  $8.5 \pm 0.61$  and the zeta potential was  $42 \pm 1.2$  as expected for a generation 6.5 dendrimer with 512 carboxyl-groups on the surface. The absence of small molecular weight impurities was confirmed by size exclusion chromatography and high performance liquid chromatography. Characterized dendrimers were subsequently evaluated for oral toxicity and translocation in mice.

### Acute oral toxicity of G6.5-COOH dendrimer

Potential toxicity of doses employed in the bioavailability studies (1 mg/kg) was evaluated in immune competent CD-1 mice in order to exclude local toxicity due to dendrimers as the cause of increased permeation and oral bioavailability. Use of an immune competent model becomes relevant with reports suggesting nanoparticle trafficking and sequestering by M-cells and Peyer's patches<sup>43</sup>. Results indicate that G6.5-COOH did not show any signs of toxicity after oral administration in CD-1 mice. Animal weights observed over ten days of the study did not show any significant differences from the control group. Various blood parameters (data not shown) also indicated no differences from the control group. The administered dose also tested negative for endotoxin contamination.

### Radiolabeling of G6.5-COOH dendrimer and characterization

In order to track the dendrimer *in vivo* it was radiolabeled with <sup>125</sup>I. <sup>125</sup>I emitting high-energy  $\gamma$ -radiation was chosen for ease of sample detection. G6.5-COOH (11  $\mu$ Ci/mg) was radiolabeled with Bolton-Hunter [<sup>125</sup>I] reagent (Supplementary Figure 1). Progression of the reaction was monitored by thin layer chromatography. After purification by dialysis and preparative size exclusion on a PD-10 column, the radiolabeled dendrimers were characterized by size exclusion chromatography (Figure 1) to confirm the absence of free <sup>125</sup>I-labeled Bolton-Hunter reagent or other small molecular weight impurities. Size exclusion profile on both the Superose 6 and PD-10 columns indicate that the radiolabeled G6.5-COOH profile had negligible quantities of small molecular radioactivity as determined by area under the curve analysis (Figure 1). Size exclusion profiles demonstrated the absence of small molecule impurities with most of the radioactivity associated with large molecular weight fraction (dendrimer elution volume).

### Stability of radiolabeled G6.5-COOH dendrimer in simulated gastric and intestinal fluids

It was important to ascertain the stability of the radiolabeled G6.5-COOH dendrimers in the gastrointestinal environment before oral administration in mice. Therefore, the stability of the radiolabeled dendrimers (G6.5COOH-<sup>125</sup>I) in simulated gastric and intestinal conditions, as inferred by the presence or absence of small molecular weight radiolabel in a size exclusion profile, was evaluated over time at 37°C. Size exclusion profile of the radiolabeled G6.5-COOH after exposure to simulated GI conditions revealed minimal release of small molecular weight radiolabel as shown in Figure 2. Samples were analyzed at three time points (1h, 4h and 12h). Results indicate that radiolabeled G6.5-COOH was relatively intact under the simulated pH and enzymatic conditions of the GI tract with large molecular weight peak corresponding to majority of area under the curve under both SGF and SIF conditions (SGF: 1h- 100%, 4h- 99.4%, 12h- 99.3% and SIF: 1h- 99.9%, 4h- 99.8%, 12h- 98.7%) (Figure 2). It is worth mentioning that over 12h under the simulated intestinal conditions there was about 1.3% release of radioactivity corresponding to small molecular weight fraction as indicated by area under the curve analysis (Figure 2). Control experiment (data not shown) with <sup>125</sup>I was performed to demonstrate the validity of the methods for differentiating small molecules and macromolecules under these specific conditions. Stability studies showed that the radiolabeled G6.5-COOH could be employed for further bioavailability studies.

### ***In-situ* stability of radiolabeled G6.5-COOH dendrimers**

The simulated conditions evaluated in the earlier section were made according to US pharmacopeia<sup>42</sup> and might vary slightly from fluids actually secreted into the mice lumen. Hence, it was decided to evaluate the stability of radiolabeled G6.5-COOH in mice lumen (1h, 4h, 12h) at 37 °C. Results demonstrate that incubation in mice intestinal lumen over time did not lead to considerable breakdown of radiolabeled G6.5-COOH dendrimers (Figure 3A). Only minimal degradation (3.5% over 4h) was observed with the appearance of small molecular weight radiolabels increasing over time (Figure 3A).

Next stability study was conducted in an *in-situ* loop perfusion setup. It was performed to evaluate if the interactions of the radiolabeled dendrimers with the dynamic layers of the intestinal serosa and mucus affects their stability. Rats were chosen, as it was easier to implement the in-situ loop method, owing to their larger size in comparison with mice. Animals (n=3) could be kept alive under anesthesia only for 2h. Results from the size exclusion profile of fluid collected from the lumen of the in-situ loop at end-point of the experiment indicate that there was very minimal release (0.2%) of the small molecular weight radiolabel, and the radiolabeled dendrimers appeared to be intact (Figure 3B).

To examine the possibility that radiolabeled dendrimers might be released in the plasma, radiolabel stability in mouse serum was evaluated. Size exclusion profile of serum containing radiolabeled G6.5-COOH incubated at 37°C for 24h revealed that there was minimal radiolabel release (5.6%) occurring due to conditions in the plasma and the large molecular weight fraction was mostly intact (Figure 3C).

### **Oral translocation of G6.5-COOH dendrimers**

Next we assessed the oral translocation of the G6.5-COOH dendrimers in CD-1 mice. A preliminary study (data not shown) indicated that the oral bioavailability of dendrimers plateaus off at about 4h, which correlated with reports of intestinal transit time in mice (varies between 2–4h<sup>44, 45</sup>). Hence all subsequent studies employed a four-hour time point to evaluate bioavailability. An investigational dose of 1 mg/kg G6.5-COOH dendrimer (earlier determined to be non-toxic) was administered by oral gavage technique to CD-1 mice (n=5) and accumulation of the dendrimer in major organs was traced by measuring the radioactivity on a  $\gamma$ -counter. Results (Figure 4) demonstrate that radiolabeled markers associated with anionic G6.5 dendrimers are absorbed orally. The radiolabeled displayed bioavailability of  $22.4 \pm 3.8\%$  (% of the administered dose) (Figure 4). 70% of the overall administered dose was recovered in these experiments. Most of the bioavailable dose had been excreted in the urine by 4h, but quantities of radioactivity did localize in organs such as the liver, kidneys, lungs and blood. To exclude the presence of free <sup>125</sup>I in systemic circulation the thyroid was examined as an internal control for accumulation of radioactivity. In all studies there was less than 0.2% of radioactive dose present.

Dose absorbed in the plasma was analyzed by size exclusion chromatography to check for the integrity of the radioactive fraction that was bioavailable (1h and 4h). Size exclusion profiles of plasma revealed the presence of both large molecular weight and to an extent small molecular weight species (Figure 5A). Control experiments showed the validity of the method employed in differentiating small molecules and large molecules in the plasma (Figure 5B). Supplementary Figure 2 also shows the size exclusion profile of <sup>125</sup>I-labeled Bolton-Hunter reagent in plasma and urine to confirm that the compound still eluted in the small molecular weight range in the presence of these fluids. Results suggest presence of a mixture of small and macromolecular species in the systemic circulation implying partial breakdown of the radiolabeled dendrimers *in vivo*. Area under the curve distribution indicated that 41.9% (4h) corresponded to large molecular weight compounds.

Urine samples were also analyzed for integrity of the radiolabeled compounds in a fashion similar to plasma experiments. It was observed that radioactivity corresponding to only small molecular weight fractions was present in all urine samples as analyzed by size exclusion chromatography (Supplementary Figure 3). This result was expected in that radiolabeled G6.5-COOH dendrimers are about 8.5nm in size and would not easily be excreted in the urine unless degraded. Radioactivity corresponding to small molecules that was observed in the plasma earlier was cleared by the kidneys over time and hence detected in the urine. An intravenous dose of radiolabeled G6.5-COOH was also administered (n=1) as a control to identify if any *in vivo* factors affected the stability of the system once it reached the systemic circulation. The plasma from mice was analyzed after 4h for integrity as mentioned earlier. Size exclusion chromatogram of the plasma profile indicates that the entire radioactivity still remained associated with the large molecular weight peak and no degradation (0%) was observed (Supplementary Figure 4). Interestingly, when the urine from the intravenous experiment was analyzed after 4h by size exclusion, the results indicate that there was substantial degradation with 76% of the area under the curve (AUC) present in small molecular weight region (Supplementary Figure 4).

A fraction of the reported 22.4% oral bioavailability reported based on radioactivity might include small molecular weight entities as shown by radioactivity profile of the plasma. The small molecular weight associated radioactivity can be generated either pre- or post-epithelial. Area under the curve (AUC) analysis revealed that 41.9% of the radioactivity profile in plasma corresponded to large molecules (Figure 5). Plasma profile was considered a reliable indicator and this distribution was scaled to the oral bioavailability numbers, results of which indicate that 9.4% of the orally administered dose could be attributed to bioavailable large molecules.

## DISCUSSION

Polymers have been examined in oral delivery applications. Polymers such as hydroxypropylmethylcellulose (HPMC) are extensively used as bulking agents in oral formulations<sup>46</sup>. Chitosan derivatives possess mucoadhesive properties and hence have been exploited in oral delivery applications as sustained release depots<sup>47, 48</sup>. The influence of size and charge on trans-epithelial transport of PAMAM dendrimers has been investigated<sup>32-34</sup>. It has been shown that attachment of lipids to PAMAM dendrimers increases transport across intestinal epithelial cells<sup>36, 49</sup>, and that endocytic uptake of dendrimers influences their paracellular transport across epithelial monolayers<sup>38</sup>. These studies however were in an *in vitro* setting. It is necessary to investigate the potential of dendrimers for oral delivery in an *in vivo* system where the pre- and post-epithelial factors play crucial roles.

In order to comprehend results from *in vivo* toxicity and oral bioavailability studies it was necessary to employ well characterized probes. G6.5-COOH dendrimers used in this study were characterized for their size, zeta potential and absence of small molecular weight impurities (Table 1). Physicochemical characteristics of the dendrimer conformed to expected trends. Acute oral toxicity evaluations at the investigational dose of 1 mg/kg showed no detectable signs of toxicity. It was important to confirm these results before evaluating oral bioavailability of the dendrimers since any toxic effects in the local GI environment could lead to an artificial increase in epithelial permeability.

After the anionic G6.5 dendrimers were radiolabeled, they were purified in order to remove the residual <sup>125</sup>I labeled Bolton-Hunter reagent or any other small molecular weight impurities. It was observed that use of a buffered solvent was necessary both during dialysis or size exclusion chromatography to achieve complete purification. The small molecular weight <sup>125</sup>I labeled impurities can easily complex or encapsulate within the dendrimers'



hollow structure, and use of saline or any buffer system is thought to disrupt these interactions, hence successfully removing any small molecular weight impurity associated with the dendrimer. The radiolabeled dendrimers were characterized by size exclusion chromatography with three successive runs of the fractionated macromolecular peaks to ensure the absence of small molecules (Figure 1), only after which these preparations were used. Area under the curve (AUC) of radiolabeled G6.5 dendrimers (both Superose 6 and PD-10 size exclusion columns) suggests negligible quantities of small molecular weight impurities (Figure 1). The elution profiles were examined for higher volumes (Figure 1A) to ensure no small molecules were retained in the column. The Superose 6 column that has a better resolution was used to confirm the results observed with the PD-10 size exclusion columns.

The simulated gastric and intestinal fluids were prepared according to US pharmacopeia recommendations<sup>42</sup>, generally used to screen drug formulations and other routine testing. Results from these stability studies suggest that the radiolabeled dendrimers were stable under these conditions (Figure 2), with minimal breakdown (< 1%) over 4h. Although the intestinal transit time in mice is about 2–4h<sup>44</sup>, a 12h time point was also investigated to understand their behavior at prolonged time points and the trend remained the same. The radiolabeled G6.5-COOH demonstrated minimal degradation probably because of the steric hindrance displayed by the carboxyl surface groups that could restrict enzymatic access.

Possible *in vivo* scenarios that could potentially cleave the radiolabel off dendrimers were tested *in-situ* such as mice intestinal secretions, the dynamic mucus and serosal layers present in mice and mice serum. None of these evaluated conditions captured breakdown to the extent seen in the *in vivo* bioavailability studies (Figure 3). Degradation of the radiolabeled dendrimers as observed in the *in vivo* bioavailability experiments could occur in scenarios that were not tested and are subjects of future investigation. For example, the interstitial region during transport from the intestinal lumen to the systemic circulation, which is known to have prevalent brush border enzymes,<sup>50, 51</sup> could potentially cleave chemical bonds. Degradation of these probes under harsh gastric condition *in vivo* is a possibility although *in vitro* stability studies under simulated gastric conditions (Figure 2) did not capture this effect. The probability of kupffer cells in the liver degrading the radiolabeled dendrimers after absorption into systemic circulation was ruled out because this scenario would be captured in the study where radiolabeled G6.5-COOH was administered intravenously in mice, but the plasma profile from this experiment showed no signs of degradation even after 4h (Supplementary Figure 4). A detailed study is warranted to examine the pre- and post-epithelial breakdown of the small molecular weight radiolabeled fragments from the dendrimers.

A trend emerging from the oral translocation studies is that the radiolabels displayed substantial bioavailability across intestinal epithelial barriers (Figure 4). Although evaluation of mechanistic aspects were beyond the scope of this manuscript, a possible explanation, besides degradation products, could be the opening of tight junctions as observed earlier with similar G3.5-COOH systems<sup>38</sup>. G6.5-COOH dendrimers have a number of surface carboxyl groups, which potentially can increase interactions with epithelial cells in turn influencing greater tight junction opening. Poly(acrylic acid)s and polyunsaturated fatty acids are known to increase paracellular transport by causing a change in intracellular calcium concentration<sup>13–16</sup>. A similar phenomenon could potentially influence the trans-epithelial transport of carboxyl-terminated dendrimers by causing a greater calcium flux leading to greater modulation of tight junction opening.

Another important factor to consider while interpreting the bioavailability results is that in our studies accumulation in the GI tract was not included in the bioavailable fraction (Figure

4). The gastrointestinal tract is a highly perfused organ and the dendrimers could localize there after absorption into the blood, or the intestinal epithelial cells could uptake these dendrimers into intracellular compartments from the lumen, which also could contribute towards the bioavailable component. Since there was not a reliable method to demarcate between bioavailable and non-bioavailable components in the GI (*in vivo*), radioactivity in the GI was regarded as non-bioavailable. This assumption may underestimate the oral bioavailability of the investigated dendrimers. Another important point to note in the biodistribution data was the rapid clearance of anionic G6.5 dendrimers from the plasma (0.25% in plasma after 4h). Modifications such as PEGylation may be incorporated in future studies in order to increase the plasma residence time of anionic dendrimers if needed<sup>52, 53</sup>.

The unusually high bioavailability numbers given the size of the dendrimers prompted us to investigate the integrity of the radiolabeled macromolecules in the systemic circulation. Plasma profile of mice administered with G6.5-COOH revealed two radioactivity peaks corresponding to both small molecular weight and large molecular weight species as detected on a size exclusion column (Figure 5). The controls shown in Figure 5 were important in ensuring that the size exclusion methods used were valid for plasma samples. As results revealed, the 22.4% bioavailability observed was not entirely macromolecular in nature but some radioactivity corresponded to small molecules present in the plasma. In order to quantify the bioavailability that can be attributed to large molecular weight dendrimers we resorted to demarcating the percentages of macromolecules and small molecules by an area under the curve analysis. Ultimately, about 42% of the oral bioavailability can be attributed to large molecular weight fraction, which puts the bioavailability for radiolabeled G6.5-COOH at 9.4% in 4h. These results support the potential of G6.5 dendrimers in delivery of bioactive agents across the gut mucosae. There have been earlier reports of radiolabels associated with dendrimers degrading under *in vivo* conditions suggesting the need for stable labeling techniques<sup>54</sup>.

In the control experiment where radiolabeled G6.5 dendrimers were administered intravenously, the urine profile analyzed by size exclusion chromatography (Supplementary Figure 4) showed that there were still small molecular weight impurities appearing in the urine, even though the plasma profile showed intact dendrimers. This observation suggests possibility of breakdown of the radiolabeled G6.5 dendrimers in other organs such as the kidneys where peptidases and other enzymes<sup>55</sup> could cleave the small molecule radiolabel present on the dendrimers. Future studies in this area include techniques to eliminate or reduce the degradation that we observed with the existing chemical bonds such as incorporation of the radioactive entity within the structure of the dendrimer, demonstrate with dendrimer-based carriers that it is possible to enhance the oral bioavailability of poorly bioavailable drugs *in vivo*, and investigate in detail the mechanisms and sites of degradation of radiolabeled dendrimers, as well as understanding the mechanisms of oral translocation and the long-term effects of dendrimer bioaccumulation.

In conclusion Figure 6 shows the major findings from this study, demonstrating the potential of anionic G6.5 dendrimers to permeate oral barriers and absorb in the systemic circulation. Systemic absorption of dendrimers after oral administration, and challenges with the instability of the radioactive labeled system upon *in vivo* evaluation in mice is presented. The estimated oral bioavailability of G6.5 dendrimers, provide opportunities for further investigation of these polymers in oral drug delivery applications.

## Supplementary Material

Refer to Web version on PubMed Central for supplementary material.

## Acknowledgments

Financial support was provided by the National Institutes of Health (R01EB007470 and R01DE019050), Utah Science Technology and Research (USTAR) initiative and a University of Utah Graduate Research Fellowship. The authors thank Dr. Rebecca Macchione and Lyssa Lambert from the Li Lab for their assistance in the *in-situ* loop procedure performed on rats.

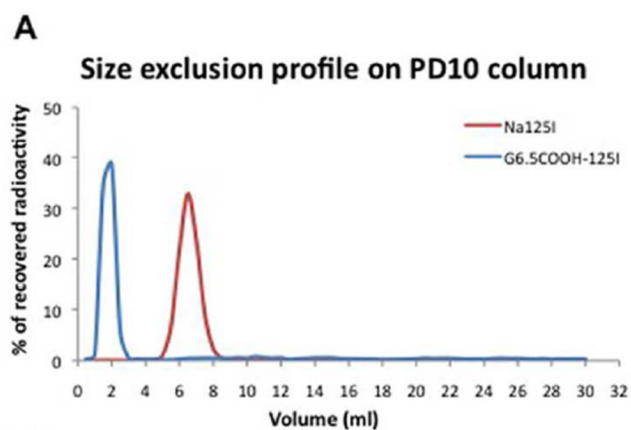
## References

1. Duncan R. Polymer conjugates as anticancer nanomedicines. *Nat Rev Cancer*. 2006; 6(9):688–701. [PubMed: 16900224]
2. Harris JM, Chess RB. Effect of pegylation on pharmaceuticals. *Nat Rev Drug Discov*. 2003; 2(3): 214–221. [PubMed: 12612647]
3. Pasut G, Guiotto A, Veronese F. Protein, peptide and non-peptide drug PEGylation for therapeutic application. *Expert Opinion on Therapeutic Patents*. 2004; 14(6):859–894.
4. Pachence JM, Belinka B, Paul Simon P. Novel methods for site-directed drug delivery. *Drug Delivery Technology*. 2003; 3(1):40–45.
5. Kopecek J, Kopeckova P, Minko T, Lu ZR, Peterson CM. Water soluble polymers in tumor targeted delivery. *J Control Release*. 2001; 74(1–3):147–158. [PubMed: 11489491]
6. Duncan R. The dawning era of polymer therapeutics. *Nat Rev Drug Discov*. 2003; 2(5):347–360. [PubMed: 12750738]
7. Jani P, Halbert GW, Langridge J, Florence AT. Nanoparticle uptake by the rat gastrointestinal mucosa: quantitation and particle size dependency. *J Pharm Pharmacol*. 1990; 42(12):821–826. [PubMed: 1983142]
8. Fasano A. Novel approaches for oral delivery of macromolecules. *J Pharm Sci*. 1998; 87(11):1351–1356. [PubMed: 9811489]
9. Cai Z, Wang Y, Zhu LJ, Liu ZQ. Nanocarriers: a general strategy for enhancement of oral bioavailability of poorly absorbed or pre-systemically metabolized drugs. *Curr Drug Metab*. 2010; 11(2):197–207. [PubMed: 20384585]
10. Ranaldi G, Marigliano I, Vespignani I, Perozzi G, Sambuy Y. The effect of chitosan and other polycations on tight junction permeability in the human intestinal Caco-2 cell line(1). *J Nutr Biochem*. 2002; 13(3):157–167. [PubMed: 11893480]
11. Yeh TH, Hsu LW, Tseng MT, Lee PL, Sonjae K, Ho YC, Sung HW. Mechanism and consequence of chitosan-mediated reversible epithelial tight junction opening. *Biomaterials*. 2011; 32(26): 6164–6173. [PubMed: 21641031]
12. Sadeghi AM, Dorkoosh FA, Avadi MR, Weinhold M, Bayat A, Delie F, Gurny R, Larijani B, Rafiee-Tehrani M, Junginger HE. Permeation enhancer effect of chitosan and chitosan derivatives: comparison of formulations as soluble polymers and nanoparticulate systems on insulin absorption in Caco-2 cells. *Eur J Pharm Biopharm*. 2008; 70(1):270–278. [PubMed: 18492606]
13. Hossain Z, Hirata T. Molecular mechanism of intestinal permeability: interaction at tight junctions. *Mol Biosyst*. 2008; 4(12):1181–1185. [PubMed: 19396381]
14. Madsen F, Peppas NA. Complexation graft copolymer networks: swelling properties, calcium binding and proteolytic enzyme inhibition. *Biomaterials*. 1999; 20(18):1701–1708. [PubMed: 10503971]
15. Shakweh M, Ponchel G, Fattal E. Particle uptake by Peyer patches: a pathway for drug and vaccine delivery. *Expert Opinion on Drug Delivery*. 2004; 1(1):141–163. [PubMed: 16296726]
16. Des Rieux A, Fievez V, Garinot M, Schneider YJ, Preat Vr. Nanoparticles as potential oral delivery systems of proteins and vaccines: A mechanistic approach. *Journal of Controlled Release*. 2006; 116(1):1–27. [PubMed: 17050027]
17. Tomalia DA, Baker H, Dewald J, Hall M, Kallos G, Martin S, Roeck J, Ryder J, Smith P. A new class of polymers: starburst-dendritic macromolecules. *Polymer Journal*. 1985; 17(1):117–132.
18. Tomalia DA, Reyna LA, Svenson S. Dendrimers as multi-purpose nanodevices for oncology drug delivery and diagnostic imaging. *Biochem Soc Trans*. 2007; 35(Pt 1):61–67. [PubMed: 17233602]

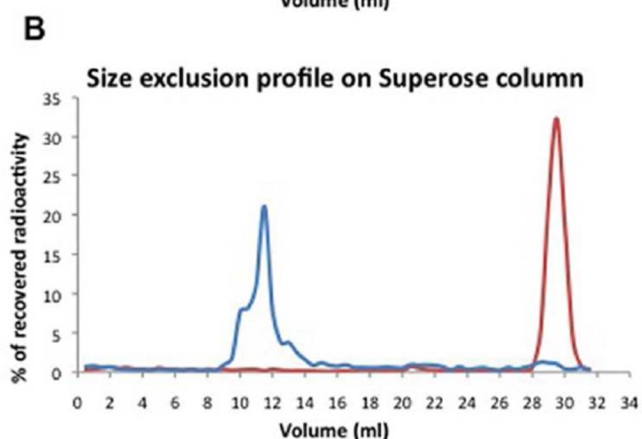
19. Menjoge AR, Kannan RM, Tomalia DA. Dendrimer-based drug and imaging conjugates: design considerations for nanomedical applications. *Drug Discov Today*. 2010; 15(5–6):171–185. [PubMed: 20116448]
20. Svenson S. Dendrimers as versatile platform in drug delivery applications. *Eur J Pharm Biopharm*. 2009; 71(3):445–462. [PubMed: 18976707]
21. Tomalia DA, Dewald JR. Dense star polymers having core, core branches, terminal groups. 1985
22. Tomalia DA. Starburst/Cascade Dendrimers: Fundamental building blocks for a new nanoscopic chemistry set. *Advanced Materials*. 1994; 6(7–8):529–539.
23. Thiagarajan G, Ray A, Malugin A, Ghandehari H. PAMAM-camptothecin conjugates inhibit proliferation and induces nuclear fragmentation in colorectal carcinoma cells. *Pharm Res*. 2010; 27(11):2307–2316. [PubMed: 20552256]
24. Tomalia DA, Naylor AM, Goddard WA. Starburst dendrimers: molecular-level control of size, shape, surface chemistry, topology, and flexibility from atoms to macroscopic matter. *Angewandte Chemie International Edition in English*. 1990; 29(2):138–175.
25. Ward BB, Dunham T, Majoros IJ, Baker JR Jr. Targeted dendrimer chemotherapy in an animal model for head and neck squamous cell carcinoma. *Journal of Oral and Maxillofacial Surgery*. 2011; 69(9):2452–2459. [PubMed: 21684654]
26. Thomas TP, Goonewardena SN, Majoros IJ, Kotlyar A, Cao Z, Leroueil PR, Baker JR. Folate-targeted nanoparticles show efficacy in the treatment of inflammatory arthritis. *Arthritis & Rheumatism*. 2011; 63(9):2671–2680. [PubMed: 21618461]
27. Malik N, Evagorou EG, Duncan R. Dendrimer-platininate: a novel approach to cancer chemotherapy. *Anticancer Drugs*. 1999; 10(8):767–776. [PubMed: 10573209]
28. Menjoge AR, Rinderknecht AL, Navath RS, Faridnia M, Kim CJ, Romero R, Miller RK, Kannan RM. Transfer of PAMAM dendrimers across human placenta: Prospects of its use as drug carrier during pregnancy. *Journal of Controlled Release*. 2011; 150(3):326–338. [PubMed: 21129423]
29. Navath RS, Menjoge AR, Dai H, Romero R, Kannan S, Kannan RM. Injectable PAMAM dendrimer, PEG hydrogels for the treatment of genital infections: formulation and in vitro and in vivo evaluation. *Molecular Pharmaceutics*. 2011; 8(4):1209–1223. [PubMed: 21615144]
30. Inapagolla R, Guru BR, Kurtoglu YE, Gao X, Lieh-Lai M, Bassett DJP, Kannan RM. In vivo efficacy of dendrimer-methylprednisolone conjugate formulation for the treatment of lung inflammation. *International Journal of Pharmaceutics*. 2010; 399(1–2):140–147. [PubMed: 20667503]
31. Wiwattanapatapee R, Carreno-Gomez B, Malik N, Duncan R. Anionic PAMAM dendrimers rapidly cross adult rat intestine in vitro: a potential oral delivery system? *Pharm Res*. 2000; 17(8):991–998. [PubMed: 11028947]
32. El-Sayed M, Ginski M, Rhodes C, Ghandehari H. Transepithelial transport of poly(amidoamine) dendrimers across Caco-2 cell monolayers. *J Control Release*. 2002; 81(3):355–365. [PubMed: 12044574]
33. El-Sayed M, Rhodes CA, Ginski M, Ghandehari H. Transport mechanism(s) of poly (amidoamine) dendrimers across Caco-2 cell monolayers. *Int J Pharm*. 2003; 265(1–2):151–157. [PubMed: 14522128]
34. Kitchens KM, Kolhatkar RB, Swaan PW, Eddington ND, Ghandehari H. Transport of poly(amidoamine) dendrimers across Caco-2 cell monolayers: Influence of size, charge and fluorescent labeling. *Pharm Res*. 2006; 23(12):2818–2826. [PubMed: 17094034]
35. Goldberg DS, Vijayalakshmi N, Swaan PW, Ghandehari H. G3.5 PAMAM dendrimers enhance transepithelial transport of SN38 while minimizing gastrointestinal toxicity. *J Control Release*. 2011; 150(3):318–325. [PubMed: 21115079]
36. Jevprasesphant R, Penny J, Attwood D, McKeown NB, D'Emanuele A. Engineering of dendrimer surfaces to enhance transepithelial transport and reduce cytotoxicity. *Pharmaceutical Research*. 2003; 20(10):1543–1550. [PubMed: 14620505]
37. Najlah M, Freeman S, Attwood D, D'Emanuele A. In vitro evaluation of dendrimer prodrugs for oral drug delivery. *Int J Pharm*. 2007; 336(1):183–190. [PubMed: 17188439]

38. Goldberg DS, Ghandehari H, Swaan PW. Cellular entry of G3.5 poly (amido amine) dendrimers by clathrin- and dynamin-dependent endocytosis promotes tight junctional opening in intestinal epithelia. *Pharm Res.* 2010; 27(8):1547–1557. [PubMed: 20411406]
39. Sadekar S, Ghandehari H. Transepithelial transport and toxicity of PAMAM dendrimers: Implications for oral drug delivery. *Advanced Drug Delivery Reviews.* 2012; 64(6):571–588. [PubMed: 21983078]
40. Greish K, Thiagarajan G, Herd H, Price P, Bauer H, Hubbard D, Burckle A, Sadekar S, Yu T, Anwar A, Ray A, Ghandehari H. Size and surface charge significantly influence the toxicity of silica and dendritic nanoparticles. *Nanotoxicology.* 2011; 6(7):718–728.
41. Malik N, Wiwattanapatapee R, Klopsch R, Lorenz K, Frey H, Weener JW, Meijer EW, Paulus W, Duncan R. Dendrimers: relationship between structure and biocompatibility in vitro, and preliminary studies on the biodistribution of 125I-labelled polyamidoamine dendrimers in vivo. *J Control Release.* 2000; 65(1–2):133–148. [PubMed: 10699277]
42. U.S. Pharmacopeia. <http://www.usp.org/> (10/18/11),
43. Shakweh M, Besnard M, Nicolas V, Fattal E. Poly (lactide-co-glycolide) particles of different physicochemical properties and their uptake by peyer's patches in mice. *Eur J Pharm Biopharm.* 2005; 61(1–2):1–13. [PubMed: 16005619]
44. Kim SK. Small intestine transit time in the normal small bowel study. *Am J Roentgenol Radium Ther Nucl Med.* 1968; 104(3):522–524.
45. Schwarz R, Kaspar A, Seelig J, Künnecke B. Gastrointestinal transit times in mice and humans measured with 27Al and 19F nuclear magnetic resonance. *Magnetic Resonance in Medicine.* 2002; 48(2):255–261. [PubMed: 12210933]
46. Qiu, Yihong; C, Y.; Liu, Lirong; Zhang, Geoff GZ.; Porter, William. Developing solid oral dosage forms: pharmaceutical theory and practice. Maryland Heights: Elsevier; 2008. Design, development, and scale-up of formulation and process.
47. Bowman K, Leong KW. Chitosan nanoparticles for oral drug and gene delivery. *Int J Nanomedicine.* 2006; 1(2):117–128. [PubMed: 17722528]
48. Elsayed A, Al-Remawi M, Qinna N, Farouk A, Al-Sou'od K, Badwan A. Chitosan–Sodium Lauryl Sulfate Nanoparticles as a Carrier System for the In Vivo Delivery of Oral Insulin. *AAPS PharmSciTech.* 2011:1–7.
49. Saovapakhiran A, D'Emanuele A, Attwood D, Penny J. Surface modification of PAMAM dendrimers modulates the mechanism of cellular internalization. *Bioconjug Chem.* 2009; 20(4): 693–701. [PubMed: 19271737]
50. Ferraris RP, Villenas SA, Diamond J. Regulation of brush-border enzyme activities and enterocyte migration rates in mouse small intestine. *Am J Physiol.* 1992; 262(6 Pt 1):G1047–G1059. [PubMed: 1352087]
51. Adibi, SA.; Kim, SK. Johnson, LR. *Physiology of Gastrointestinal Tract.* New York: Raven Press; 1981. Peptide absorption and hydrolysis; p. 1073-1095.
52. Wolinsky JB, Grinstaff MW. Therapeutic and diagnostic applications of dendrimers for cancer treatment. *Adv Drug Deliv Rev.* 2008; 60(9):1037–1055. [PubMed: 18448187]
53. Kojima C, Regino C, Umeda Y, Kobayashi H, Kono K. Influence of dendrimer generation and polyethylene glycol length on the biodistribution of PEGylated dendrimers. *International Journal of Pharmaceutics.* 2010; 383(1–2):293–296. [PubMed: 19761822]
54. Boyd BJ, Kaminskas LM, Karellas P, Krippner G, Lessene R, Porter CJH. Cationic poly-l-lysine dendrimers: pharmacokinetics, biodistribution, and evidence for metabolism and bioresorption after intravenous administration to rats. *Molecular Pharmaceutics.* 2006; 3(5):614–627. [PubMed: 17009860]
55. Kenny AJ, Maroux S. Topology of microvillar membrane hydrolases of kidney and intestine. *Physiological Reviews.* 1982; 62(1):91–128. [PubMed: 6119713]



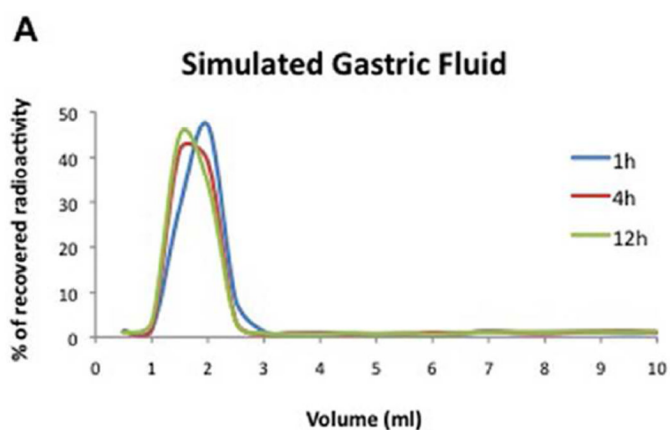


Sample	PD10 Column			
	Na <sup>125</sup> I		G6.5COOH- <sup>125</sup> I	
Volume (ml)	0.5-3.0	4.7-8.5	0.6-3.1	6.0-10.0
% Area under curve (AUC)	0.0	100	99.4	0.43

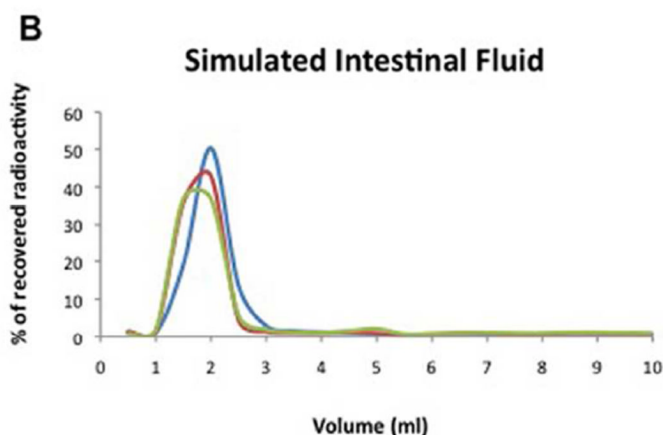


Sample	Superose Column			
	Na <sup>125</sup> I		G6.5COOH- <sup>125</sup> I	
Volume (ml)	1.3-2.5	27.9-31.4	8.7-22.8	27.3-30.0
% Area under curve (AUC)	0.23	99.5	95.5	3.3

**Figure 1.** Size exclusion profile of radiolabeled PAMAM dendrimers. G6.5COOH-<sup>125</sup>I dendrimers were characterized for absence of small molecular weight impurities by eluting on: A) PD-10 column and, B) Superose 6 column. Profiles indicate radioactivity patterns measured on a  $\gamma$ -counter. Tables indicate the % area under the curve (AUC) for the peaks. Na<sup>125</sup>I was eluted as a control small molecular weight radioactive compound.



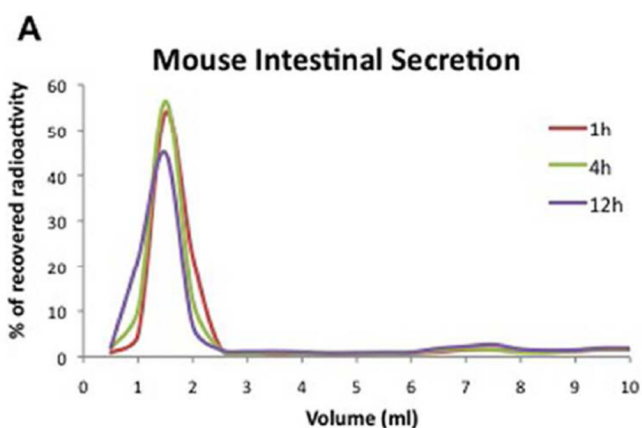
Sample	Simulated Gastric Fluid					
	1h		4h		12h	
Volume	0.5-3.0	6.9-7.1	0.5-2.9	8.5-9.9	0.5-3.0	7.0-10.0
% Area under curve (AUC)	100	<0.1	99.4	0.6	99.3	0.7



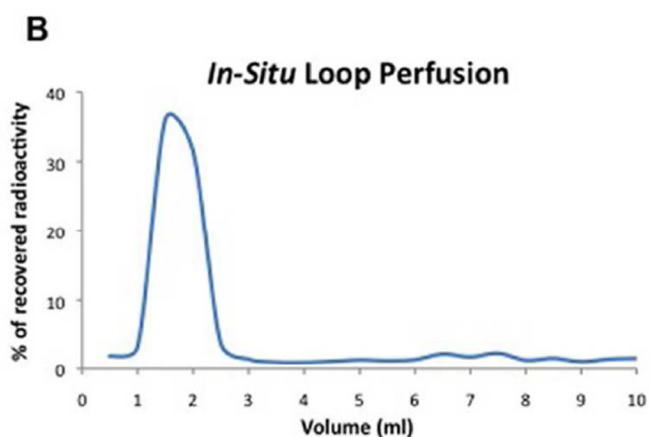
Sample	Simulated Intestinal Fluid					
	1h		4h		12h	
Volume	0.5-4.7	8.4-9.1	0.5-3.4	4.2-4.8	0.5-5.5	6.4-10.0
% Area under curve (AUC)	99.9	<0.1	99.8	0.12	98.7	1.3

**Figure 2.**

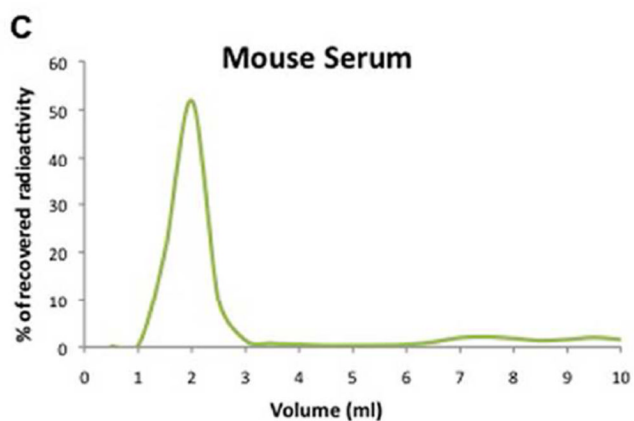
Stability profile of radiolabeled PAMAM dendrimers in simulated gastric and intestinal fluids. G6.5COOH-<sup>125</sup>I was incubated in simulated gastric and intestinal fluids containing enzymes at 37° C, and their stability over time (1h, 4h and 12h) was evaluated by size exclusion chromatography. Graph showed compounds were relatively stable under these conditions with minimal degradation observed over time. Tables indicate the % area under the curve (AUC) for the peaks.



Sample	Mouse Intestinal Flushing					
	1h		4h		12h	
Volume	0.5-3.0	6.3-10.0	0.5-2.8	6.1-10.0	0.5-4.0	6.0-10.0
% Area under curve (AUC)	96.8	3.2	96.5	3.5	91.4	8.6



Sample	<i>In-Situ</i> Loop Perfusion	
Volume	0.6-2.9	6.4-7.6
% Area under curve (AUC)	99.8	0.2



Sample	Mouse Serum	
Volume	1.0-3.3	6.5-10.0
% Area under curve (AUC)	94.4	5.6

**Figure 3.** Stability of radiolabeled G6.5-COOH dendrimers evaluated under various *in-situ* conditions as analyzed by size exclusion chromatography. A) Stability of the compound in mice intestinal secretions indicated minimal release of small molecular weight impurities over time (1h, 4h and 12h). B) Stability of radiolabeled G6.5-COOH after 2h of exposure in the rat *in-situ* loop perfusion model also indicated minimal release. C) Stability of the radiolabeled compound in mice serum over 24h showed intact large molecular weight radiolabeled dendrimers. Na<sup>125</sup>I was tested as a control small molecule. Tables indicate the % area under the curve (AUC) for the peaks.

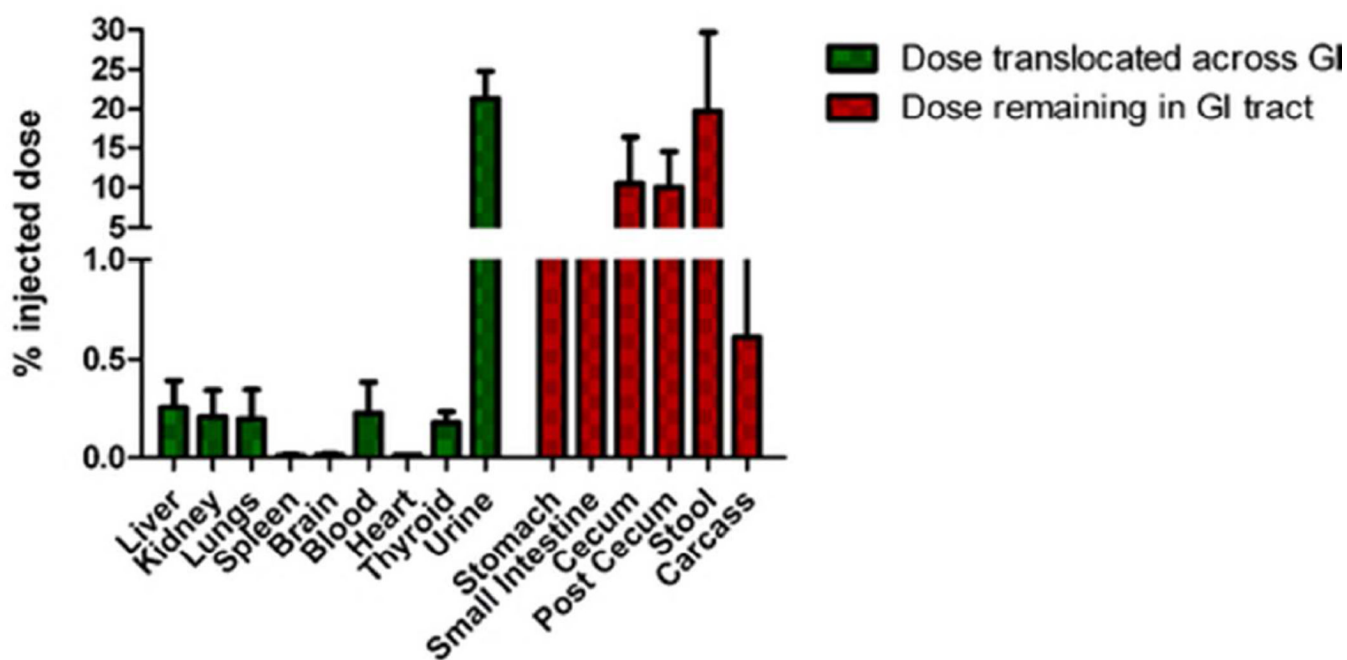
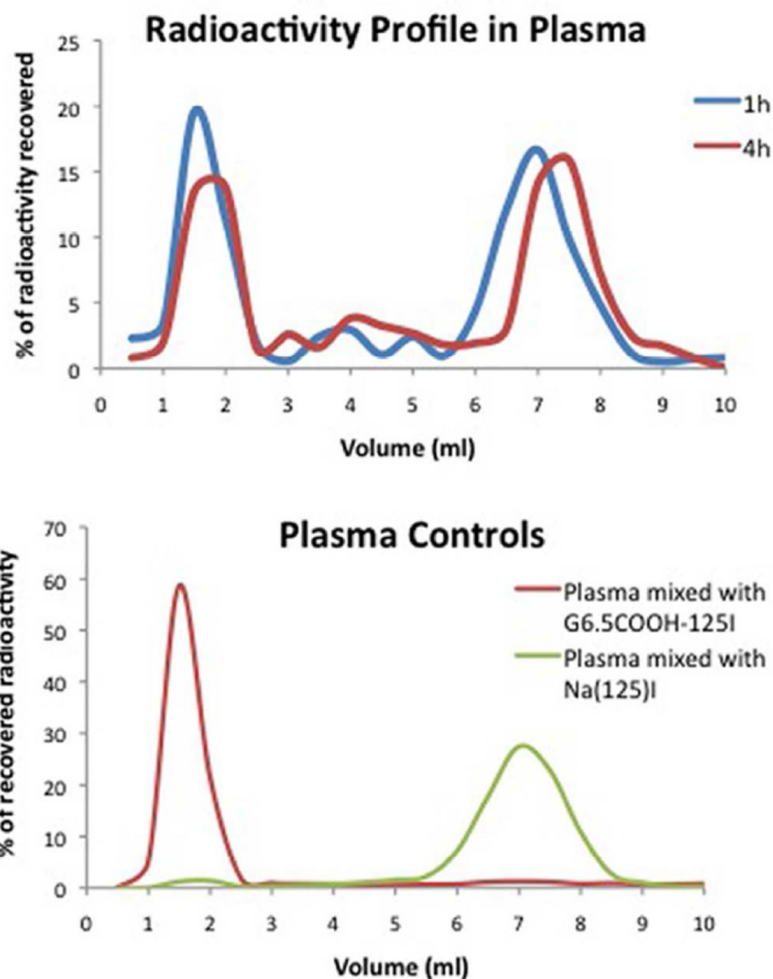


**Figure 4.** Biodistribution of orally administered anionic G6.5 dendrimers in CD-1 mice. Anionic dendrimers effectively translocated oral barriers to be absorbed into systemic circulation. 70% recovery of radioactivity was observed in these experiments.

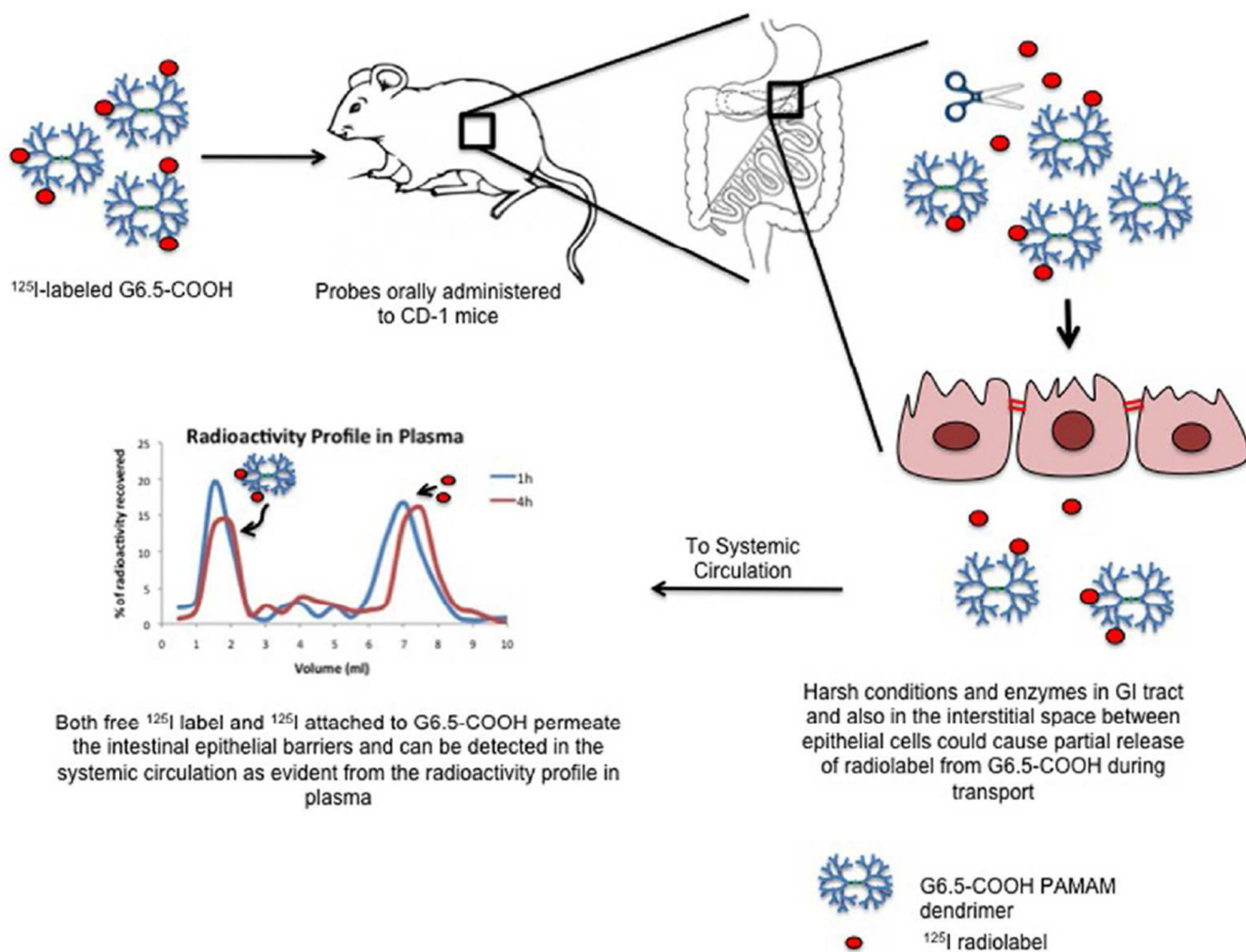


Sample	Plasma Profile (1h)		Plasma Profile (4h)	
	Volume (ml)	1.0-2.4	5.9-8.1	1.1-2.4
% Area under curve (AUC)	44.42	55.58	41.91	58.09

**Figure 5.**

A) Radioactivity profile in plasma of CD-1 mice after oral administration of G6.5-COOH as analyzed by size exclusion chromatography. Results indicate presence of large molecular weight fractions corresponding to dendrimers in plasma at 1h and 4h as well as presence of small molecular weight radioactive fractions. B) Panel indicates control graphs of small molecular weight impurities and macromolecules mixed externally with mice serum to validate the size exclusion method. Table indicates the % area under the curve (AUC) for the peaks.





Both free  $^{125}\text{I}$  label and  $^{125}\text{I}$  attached to G6.5-COOH permeate the intestinal epithelial barriers and can be detected in the systemic circulation as evident from the radioactivity profile in plasma

**Figure 6.** Schematic showing the fate of radiolabeled G6.5 dendrimers in the gastrointestinal tract and evidence of its subsequent systemic absorption.

**Table 1**

Physicochemical characterization of G6.5-COOH dendrimers

Dendrimer	G6.5-COOH	Size Exclusion Profile <sup>#</sup>
# Of surface groups <sup>§</sup>	512	
Size (diameter) in nm	8.5 ± 0.61	
Zeta potential (mV) <sup>□</sup>	-42.0 ± 1.2	

<sup>§</sup> Provided by manufacturer<sup>□</sup> Zeta potential was measured at pH 7.4 (not buffered), 25°C<sup>#</sup> Profile was generated on a Superose 6 column, eluent – PBS: Acetonitrile (80:20)